Author(s): M.J. Chappell, N.D. Evans, R.J. Errington, I.A. Khan, L. Campbell, R. Ali, K.R. Godfrey, P.J. Smith
Article Title: A coupled drug kinetics-cell cycle model to analyse the response of human cells to intervention by topotecan
Year of publication: 2008

Link to published article:
http://dx.doi.org/10.1016/j.cmpb.2007.11.002

Publisher statement: None (Pre-print)

A COUPLED DRUG KINETICS - CELL CYCLE MODEL TO ANALYSE THE RESPONSE OF HUMAN CELLS TO INTERVENTION BY TOPOTECAN

M. J. Chappell* (†), N. D. Evans*,
R. J. Errington***, I. A. Khan****, L. Campbell**, R. Ali *
K. R. Godfrey* and P. J. Smith**

* School of Engineering, University of Warwick, Coventry CV4 7AL, U.K.
** Department of Pathology, Wales College of Medicine, Cardiff University, Cardiff CF14 4XN, U.K.
*** Department of Medical Biochemistry, Wales College of Medicine, Cardiff University, Cardiff CF14 4XN, U.K.

**** Biostatistics and Bioinformatics Unit

Cardiff University, Cardiff, CF14 4XN

Abstract: A model describing the response of the growth of single human cells in the absence and presence of the anti-cancer agent topotecan (TPT) is presented. The model includes a novel coupling of both the kinetics of TPT and cell cycle responses to the agent. By linking the models in this way, rather than using separate (disjoint) approaches, it is possible to illustrate how the drug perturbs the cell cycle. The model is compared to experimental *in vitro* cell cycle response data (comprising single cell descriptors for molecular and behavioural events) – showing good qualitative agreement for a range of TPT dose levels.

Keywords: Drug kinetics, cell cycle models, compartmental models, topotecan.

(†) Author for Correspondence

1. INTRODUCTION

In this paper, an approach is described in which a coupled mathematical model has been developed that is capable of describing the *in vitro* drug kinetics of the anti-cancer agent topotecan (TPT) for single human osteosarcoma cells linked to primary biological (cell cycle) responses. The model offers the possibility of demonstrating both the dynamic and temporal interactions of active drug delivered to its DNA-associated molecular target and the downstream impact on cell growth and death. Live-cell data generated from new experimental procedures have been used and these procedures were developed to meet the demands of model comparison/validation [1]. In order to do this a series of robust quantitative laboratory assays have been designed to track and measure time-integrated events at the single cell level. Acquired data are used for parameter estimation and model simulation to further investigate the interactions of the drug with its target and possible routes for cellular evasion of drug action (i.e. drug resistance). The aim of this study was to assess the possibility of linking an existing drug kinetic model (for TPT) with a basic model for cell cycle dynamics [2]. Ultimately, a robust and validated version of such a generic model could be used to design and predict the consequences and potential failure of drug treatment regimens.

In Section 2 an outline of coupled drug kinetic – cell cycle response modelling and the underlying biochemistry for TPT is provided. The mathematical model developed is described in Section 3 and the methods for data collection and database generation are given in Section 4. The parameter estimation approach is presented in Section 5. Results from the parameter estimation using the experimental data are provided in Section 6.

2 BACKGROUND

2.1 Coupled Drug Kinetics/Cell Cycle Response Modelling

In general the relationships between drug kinetics and the drug's effect on the cell cycle are extremely complicated, especially when the perturbed biological system being modelled expresses discrete events within a heterogeneous cellular population. The linking of drug kinetics and cell cycle models to describe the kinetics for heterogeneous cell populations is relatively new. A recent model, developed independently by Alarcón

et al. [3] considers an approach that uses the cell cycle as a descriptor of the biological response. A current drawback is the difficulty in obtaining model validation or comparison with experimental data.

Critical to the modelling of the cell cycle responses to the action of topotecan is the ability to undertake high temporal resolution monitoring of cell cycle progression enabling the tracking of a single cell in a non-invasive manner even within heterogeneous populations. The green fluorescent protein (GFP)-based probe has expression, location and destruction characteristics that shadow cyclin B1 dynamics in living cells [4]. The non-perturbing stealth reporter performance has been validated on high content to high throughput detection platforms comprising multi-well high-throughput screen (HTS) imaging, single cell kinetic-tracking and multi-parameter flow cytometry [4, 5]. Cyclin B1-GFP tracking provides sub-phase information on cell cycle progression in parallel with morphological landmarks and DNA content analysis (Figure 1a). The continuous progression of cell cycle traverse and encoded molecular readouts in cell lineages (Figure 1b) has been tracked, enabling the extraction of data with subsequent linking to the phenotypic cellular behaviour in response to topotecan treatment. These experimental data provide the fundamental information upon which the coupled drugs - cell cycle model is both developed and confirmed.

(Figure 1 in here)

2.2 Introduction to TPT: Action of the drug

The anti-cancer agent considered here is TPT. It was selected on the basis of the experimental and clinical evidence for its primary cytotoxic activity against lung, breast and ovarian cancers [6]. TPT is a water-soluble derivative of camptothecin (CPT), an alkaloid isolated from the tree *camptotheca acuminata*, and acts as a DNA topoisomerase I, (topo I), inhibitor [7]. Topo I is a nuclear enzyme involved in DNA replication and repair. The enzyme unwinds supercoiled double stranded DNA (dsDNA) by temporarily binding to and cleaving one of the strands, forming a ‘cleavable complex’. DNA cleavage and ligation reactions catalysed by the enzyme are tightly controlled and are normally

barely detectable. The cleavage is coupled with religation to restore continuity to the DNA complex (Figure 2(a)). In the presence of TPT, the cleaved DNA-topo I complex is stabilised, effectively inhibiting religation and resulting in accrual of complexes each sequestering a strand-break (Figure 2(b)). The drug-induced single-strand breaks are reversible upon drug removal since the drug is non-covalently associated with DNA in forming the cleavable complex. Such lesions are considered non-toxic as they can be easily repaired/reversed. However, as replication proceeds double-strand breaks can be generated by the collision of a replication fork with the trapped complex – these lesions being responsible for the primary cytotoxic effects of TPT.

(Figure 2 in here)

TPT is of particular interest since the agent has intrinsic specificity for the DNA replication period in terms of the origin of drug responses and in terms of the growth and division cycle for outcomes (Figures 3 and 4). The mammalian somatic cell cycle comprises four distinct phases. In G1, the chromosomes are unreplicated and the cell is uncommitted to division. During transition from this phase to S phase the cell commits to replication if DNA integrity is not compromised. DNA is then replicated and paired chromatids form. This is followed by the G2 phase where chromosomal material is prepared by the surveillance of its integrity (e.g. persistence of double-strand breaks sensed at a checkpoint) prior to commitment to mitosis. In M phase the nuclear membrane is lost, chromatin condenses and sister chromatids are separated with each daughter cell receiving a copy of each. Subsequently, the diploid 2n complement of chromosomes decondense in each daughter cell and the nuclear membrane is re-formed as cytokinesis is completed. The processes involved are distinct and tightly regulated both temporally and spatially [8]. For modelling purposes the cell cycle may be thought of as comprising two alternative states: G1 and S-G2-M separated by irreversible *Start* and *Finish* transitions, as defined by Tyson and Novak [2]. *Start* is defined as where the cell begins replication and *Finish* where the DNA replication is complete. *Finish* cannot occur if there have been any problems with DNA replication or chromosome alignment (Figure 4). Since TPT is believed to be S-phase specific many cells may resist the agent's

effects by failing to enter S phase (i.e. attempt to replicate DNA) during a finite exposure [9]. Blocking entry to S-phase halts the expansion of the cell population (i.e. cytostasis) and under some conditions can cause cell death (i.e. apoptosis).

(Figure 3 in here)

(Figure 4 in here)

3. THE COUPLED DRUG KINETICS-CELL CYCLE MODEL

Figure 5 provides a schematic for the coupled drug kinetics – cell cycle model. Separate models have been developed for the cell cycle and drug kinetics. These both contain the relevant basic physiology and biochemistry and are coupled together in such a manner that it is possible to illustrate how the drug perturbs the cell cycle. The TPT kinetics model describes the chemical reactions and partitions that occur when the drug moves from the medium, cytoplasm and then nuclear compartments. The active, closed-ring (lactone) form of TPT (TPT-L) undergoes reversible hydrolysis to an open-ring (hydroxy acid) form (TPT-H). This reaction is pH-dependent: the active and inactive forms predominate at low pH (<4) and high pH (>10) respectively [10].

(Figure 5 in here)

The same notation used by Evans *et al.* [11] is adopted, where concentrations of TPT-L and TPT-H are defined by *L* and *H* with subscripts, *m, e, c* and *n* defining the medium, extracellular, cellular and nucleic regions respectively. It is assumed that: (i) all the drug in the nucleus is bound and only TPT-L binds to DNA, and (ii) elsewhere reversible, pH-dependent hydrolysis occurs. The latter is modelled using an elementary linear two-compartment model, where rate constant k_{om} defines the ring opening for TPT-L and k_{cm} the ring closing for TPT-H. In the cytoplasm the corresponding rate constants are k_{oc} and k_{cc} respectively. The mixing between the medium and extracellular regions is modelled

by first-order flows. The parameter k_{mi} refers to the flow into the extracellular region from the medium and k_{mo}, the flow out of the extracellular region into the medium. The flow between the extracellular and cytoplasm is also modelled as first-order. Note that only TPT-L crosses the plasma membrane (as observed experimentally). The rate at which TPT-L binds to DNA is assumed proportional (with rate constant, k_b), to the product of the concentration of TPT-L in the cytoplasm, $L_c(t)$ and free binding sites $B_F(t)$. The parameter B_T denotes the total concentration of available DNA binding sites, and, by mass conservation, the concentration of free sites is given by $B_F(t) = B_T - L_n(t)$, where $L_n(t)$ is the instantaneous concentration of bound drug. Dissociation of bound drug is assumed to be linear with rate constants k_{dl} or k_{dh} for TPT-L and TPT-H respectively. The set of ODEs describing the system is given by:

$$
\begin{aligned}
\frac{\mathrm{d}L_m}{\mathrm{d}t} &= -\left(k_{om} + k_{mi}\right) L_m + k_{cm} H_m + k_{mo}\nu_o L_e \\
\frac{\mathrm{d}H_m}{\mathrm{d}t} &= k_{om} L_m - \left(k_{cm} + k_{mi}\right) H_m + k_{mo}\nu_o H_e \\
\frac{\mathrm{d}L_e}{\mathrm{d}t} &= \frac{k_{mi}}{\nu_o} L_m - \left(k_{mo} + k_{om} + k_i\right) L_e + k_{cm} H_e + \frac{k_e}{\nu_1} L_c \\
\frac{\mathrm{d}H_e}{\mathrm{d}t} &= \frac{k_{mi}}{\nu_o} H_m + k_{om} L_e - \left(k_{cm} + k_{mo}\right) H_e \\
\frac{\mathrm{d}L_c}{\mathrm{d}t} &= k_i \nu_1 L_e - \left(k_e + k_{oc}\right) L_c + k_{cc} H_c + k_{dl}\nu_2 L_n - k_b \left(B_T - L_n\right) L_c \\
\frac{\mathrm{d}H_c}{\mathrm{d}t} &= k_{oc} L_c - k_{cc} H_c + k_{dh}\nu_2 L_n \\
\frac{\mathrm{d}L_n}{\mathrm{d}t} &= \frac{k_b}{\nu_2}\left(B_T - L_n\right) L_c - \left(k_{dl} + k_{dh}\right) L_n
\end{aligned}
\qquad (1)
$$

where $\nu_0 = V_e / V_m$, $\nu_1 = V_e / V_c$, $\nu_2 = V_c / V_n$, and V_m, V_e, V_c and V_n denote the volumes of the extracellular location (V_e) to drug medium (V_m), extracellular location to cytoplasm (V_c) and nucleus (V_n) to cytoplasm. The cellular volumes correspond to the total volume for each cell type, where it is assumed, for simplicity, that these volumes are the same

across cell types. The total volume, V_T, of the medium is equal to the sum of the volumes of the medium and extracellular location,

$$\text{i.e., } V_T = V_m + V_e = \frac{V_e}{v_0} + V_e = \frac{V_e\ 1+v_0}{v_0}.$$

The drug is administered as a bolus injection of active form only into the medium at time $t = 0$ (to give a concentration of D μM with respect to the total volume, V_T) and so the initial conditions for the model are given by:

$$L_m(0) = (1+v_0)D$$

and

$$H_m(0) = L_e(0) = H_e(0) = L_c(0) = H_c(0) = L_n(0) = 0. \qquad (2)$$

The pH level at which the experiments were undertaken was 7.2. Estimated values for the drug kinetics model parameters are provided in [11].

After one hour the medium is exchanged for drug-free medium (*washout*) and the cell tracking begins. To model *washout* at $t = 1$ h the variables relating to drug in the medium are instantaneously set to 0, that is:

$$L_m(1) = H_m(1) = L_e(1) = H_e(1) = 0. \qquad (2A)$$

All other variables within the drug kinetic model are unaffected by this event.

The drug kinetics model is coupled to the cell cycle model as shown in Figure 4. The coupling between Cyclin B1 and bound TPT in the nucleus is constrained to only have an effect in the S-G2-M state of the cell cycle process. Following the approach of Tyson and Novak [2] (for the synthesis of Cdc20) this constraint is achieved via the incorporation of a suitable Hill function in the relevant governing equation. The coupling involves a signal transduction cascade by which phosphorylation changes in the chromatin environment indicate the magnitude and persistence of lesions. Damage induces genomic stress response pathways, with negative feedback controls, that engage inhibitory pathways for halting cell cycle progression though master cell cycle regulators. Here the drug kinetics model has been linked to the master cell cycle regulators via a theoretical damage variable ([Dam]), which is itself driven by the kinetic model within the cell cycle state constraint. Later generations of the integrated model will focus on the exact nature of the stress-signalling linkage. The basic cell cycle model used is one that is

regulated by the interaction of cyclin dependent kinases (Cdks) and cyclin B1 with the Anaphase Promoting Complex (APC) group of proteins. Accordingly, APC negates Cdk activity by degrading the major mitotic cyclin (cyclin B1) while Cdk/Cyclin B1 inhibits APC activity. With regard to the cell cycle, at G1, Cdk activity is low and cyclin B1 is rapidly degraded. At *Start*, cyclin B1 levels are promoted. Cdk levels rapidly rise and are maintained through S, G2 and M (see Figure 6). At *Finish*, APC proteins are activated and specific proteins degraded.

(Figure 6 in here)

APC consists of polypeptides and auxiliary proteins: Cdc20 and Cdh1 which are key to targeting and marking those proteins that are to be degraded at the end of M to allow the system to return to G1. Cdc20 and Cdh1 are controlled differently by cyclin B which activates other features in the model. The model equations are based upon those of Tyson and Novak [2] describing mechanisms occurring in yeast cells. The system of equations employed in our model is a modified version of these based upon the action of TPT and using appropriate parameter values derived from live osteosarcoma cell data obtained from our experiments (see Section 4).

At the core of the cell cycle model are the equations governing the behaviour of Cyclin B with Cdh1. The core equations governing interaction of Cyclin B with Cdh1, in the presence of TPT, are given by:

$$\frac{\mathrm{d}[\mathrm{CycB}]}{\mathrm{d}t} = k_1 - \left(k_2' + k_2''[\mathrm{Cdh1}] + k_2'''[\mathrm{Dam}]\right)[\mathrm{CycB}] \tag{3A}$$

$$\frac{\mathrm{d}[\mathrm{Cdh1}]}{\mathrm{d}t} = \frac{k_3' + k_3''[\mathrm{Cdc20_A}]\,(1-[\mathrm{Cdh1}])}{J_3 + 1 - [\mathrm{Cdh1}]} - \frac{k_4 m[\mathrm{CycB}][\mathrm{Cdh1}]}{J_4 + [\mathrm{Cdh1}]} \tag{3B}$$

$$\frac{\mathrm{d}m}{\mathrm{d}t} = \mu m\left(1 - \frac{m}{m_*}\right) \tag{3C}$$

$$\frac{\mathrm{d}[\mathrm{Dam}]}{\mathrm{d}t} = k_{11}\,(1-[\mathrm{Dam}])\,\frac{[L_n]\,(m[\mathrm{CycB}]/J_5)^4}{1 + (m[\mathrm{CycB}]/J_5)^4} \tag{3D}$$

where the components in the square brackets refer to concentrations, m represents the mass of the cell, m_* is the maximum size to which a cell can grow, μ is the specific growth rate, k_i s are rate constants and J_i s are relevant Michaelis-Menten constants. In addition, when [CycB] falls below a certain threshold (taken to be 0.1 [2]) cell division occurs so that $m \rightarrow m/2$. It is assumed that the reaction between TPT and topo I is instantaneous, (as observed experimentally), and the level of the latter is constant. Values for the parameters are defined in Table 1. These are characterised by those given in Tyson and Novak [2] and have been appropriately scaled with respect to time according to the live-cell data provided from our experiments.

4. EXPERIMENTAL DATA COLLECTION AND DATABASE GENERATION

Generation of single-cell experimental data for cyclin B1 dynamics and incorporation into a database has provided the necessary resources for model validation/parameter estimation. High-resolution fluorescence cell tracking was performed with cells seeded into a multi-well coverslip-bottomed plate. Each well represents a different treatment regimen (a dose range for TPT 1-10 μM bolus for 1 h). The cultured dishes were placed onto a time-lapse instrument designed to capture transmission phase and cyclin B1-GFP fluorescence images. Sequences were captured every 20 min for 48 h, in triplicate per treatment regime.

At the end of the experiment the images were stacked and saved in *.stk or *.AVI format. FluroTRAK [12], an in-house software package written in Perl and developed by the Cardiff co-authors, was used to link and interact with commercial image analysis software, Metamorph (Molecular Devices Ltd, UK), to encode and transform the images into a parameterised database (see Figure 7a). The implementation of the lineage databases can be found at http://biodiversity.cs.cf.ac.uk/cymart/. CyMART provides the home for a number of databases where the core concept is to develop a bioinformatics environment where analysis tools efficiently encode microscopy images into numbers and deposit the encoded data in relational databases.

A typical time-lapse microscopy image sequence shows cells traversing the cell cycle and fluorescence changes as the cell progresses to mitosis from G1, individual cells ramp up cyclin B1-GFP expression (become brighter), and a translocation event (cytoplasm to nucleus) occurs just before mitosis. A typical cell lineage over 48 h illustrates a simple progression of a progenitor cell (B) dividing into two daughter cells and cellular information at two levels (i) phenotypic behaviour (division represented by M) and (ii) fluorescence reporter readout (cyclin B1-GFP, hence cell cycle position) at the single cell level. The lineage shown in Figure 7a consists of three overlapping and inter-related tracks. The continuous cell cycle progression between the two landmarks, represented by mitotic events (M1 to M2) at either end, was demonstrated for a typical cell originally in G2. The continuous cyclin B1 GFP-track was similarly extracted for single cells in G2 treated with 0, 0.1, 1.0 and 10 μM topotecan concentrations (Figure 7b). The principal effect was an extension between the two mitotic landmarks, and an increase in intermitotic time, including an extended delay in G2 for the cell treated with 10 μM TPT.

(Figure 7 in here)

5. MODEL PARAMETER ESTIMATION

Using estimated drug kinetics model parameters [11] the FACSIMILE software package (MCPA Software, UK) was used to fit the coupled drug kinetics-cell cycle model to the GFP fluorescence data. This computer-modelling tool is designed to numerically solve differential equations, with a particular focus on modelling the kinetics of physical and chemical systems. A particular advantage of this package is the robust numerical integrator that is able to handle stiff systems, that is, systems with widely varying rate constants (a property of the coupled model). The numerical integrator can solve all the ordinary differential equations of the model simultaneously and uses the parameter-fitting option available to fit the simulated output of the model to the experimental data. The result of this optimisation process is the estimation of the model parameters.

Parameter estimation is treated as an optimisation problem in which a given performance index, measuring overall closeness of fit, is minimised. This closeness of fit is measured

by the residual sum of squares (RSS), that is, the sum of the squared errors (between the model and the experimental data) at each time point making the optimisation a least squares problem. In FACSIMILE the RSS is given by:

$$RSS = \sum_{j=1}^{n} \left(\frac{y_{\text{obs}}(j) - y_{\text{sim}}(t_j)}{\sigma} \right)^2 \tag{4}$$

where $y_{\text{sim}}(t_j)$ is the model output at the j^{th} sampling time (t_j) and $y_{\text{obs}}(j)$ is the corresponding experimental data point. An estimate for the standard error for the output is provided by $\sigma = e \cdot R$, in which $e = 0.1$ is the estimated overall accuracy of the data (an assumed overall error of 10%) and R is the range for $y_{\text{sim}}(t_j)$ [13]. This approach is also referred to as a weighted least squares method as the random error at each sampling time t_j is multiplied by a constant weight, $1/\sigma^2$, resulting in normalisation of the residuals if σ can be chosen to be the standard deviation for the random errors.

For this study the model output, $y_{\text{sim}}(t)$, is taken to be a linear function of cyclin B concentration, [CycB], that is

$$y_{\text{sim}}(t) = \alpha[\text{CycB}] + \beta \tag{5}$$

and the observation parameters α and β are estimated from the experimental data. Since the live cells are being tracked in time these parameters are permitted to change (if appropriate) at cell division, but remain constant during an individual cell cycle. The only other parameters estimated from the live-cell data are those relating to the kinetic-cell cycle linking, namely, k_2''' and k_{11}, which are permitted to change with dose but are otherwise constant.

Confidence levels provide a statistical measure of how well the parameters are defined by the model and the data. FACSIMILE works in terms of internal parameters that are the natural logarithms of the given model parameters. Information is also returned on the estimated correlation between the estimated parameters and the standard deviation of the natural logarithm (SDLN) of each of the well-determined parameters, $\boldsymbol{p}^0$, which is estimated from the variance-covariance matrix of $\boldsymbol{p}$-$\boldsymbol{p}^0$ [13].

6. RESULTS

The parameter values and estimated parameter values, with estimates for their confidences are provided in Table 1. The plots shown in Figure 8 show three typical traces for the growth of a cell in the absence and presence of 1 and 10μM TPT. The live-cell data are denoted by the grey circles and the simulated data by the solid black curve.

(Table 1 in here)

(Figure 8 in here)

The model predicts when cell division occurs since this corresponds to the transformation in the cell mass variable $m \rightarrow m/2$ (when [CycB] drops below a given threshold, in this paper 0.1) that is preceded by the spikes in the data. As the cell divides the growth of either one of its daughter cells can be monitored. The corresponding simulation shows a good qualitative representation of the experimental data, even for the cases where TPT has been administered (Figures 8 (b) and (c)). A key feature of the estimation is that the main cell cycle parameters are fixed across doses at scaled (with respect to time) values of those used by Tyson and Novak [2]. In virtually all cases the estimated parameters have low SDLNs corresponding to high confidence in their values. The one exception corresponds to the G2 phase of the second-generation daughter cell in Figure 8(c) and is due to the low signal-to-noise ratio in the experimental data.

From Figure 8 it can be seen that the drug extends the overall time between mitoses. The main outcome from the model is obtaining the correct time-event characteristics successfully. It is noted that the model under predicts the spikes in the experimental data. However, these spikes correspond to morphological changes in the cell during mitosis. As the cell grows, its shape changes and just before division the cell ‘rounds up’ becoming spherical in shape. The light reflected back, a measure of the fluorescence, is at its most intense at this stage resulting in a false peak in the data. The parameter estimation attempts to allow for this by capping the data at some chosen fixed level.

7. CONCLUDING REMARKS

A coupled, drug kinetics – cell cycle model with the relevant cell biochemistry has been developed to describe cell regulation with time. The model provides novel linking between existing drug kinetic and a cell cycle models and is able to describe the effect that varying doses of TPT have on cell growth. Model simulations have been compared with live-cell experimental data and found to give good qualitative agreement. In addition, in virtually all cases the unknown model parameters were estimated to a high level of confidence. The close qualitative agreement between model and experimental data was obtained by estimating only those parameters that are associated with the coupling or observation of the system.

The next step is to extend the model across different cell lineages and different treatment scenarios to provide greater robustness and validation. Such a robust and well-validated model could ultimately be used to test scenarios applicable for drug treatment and design, for example, introducing delayed response characteristics. In addition, this will extend the field of application for the generic model developed.

The authors gratefully acknowledge the Biotechnology and Biological Sciences Research Council, (EBS subcommittee), for their kind support under Grant No. 88/E19305.

REFERENCES

[1] Errington, R. J., S. M. Ameer-Beg, B. Vojaovic, L. H. Patterson, M. Zloh and P. J. Smith. Advanced microscopy solutions for monitoring the kinetics and dynamics of drug-DNA damage-activated G2 checkpoint. *Adv. Drug Deliv. Rev.*, **57**, (2003), 153–167.

[2] Tyson, J. J. and B. Novak. Regulation of the eukaryotic cell cycle: molecular antagonism, hysteresis and irreversible transitions. *J.Theor. Biol.*, **210**, (2001), 249–263.

[3] Alarcón, T., H. M. Byrne and P. K. Maini. A mathematical model of the effects of hypoxia on the cell cycle of normal and cancer cells. *J. Theor. Biol.*, **229**, (2004), 395–411.

[4] Thomas N, Kenrick M, Giesler T, Kiser G, Tinkler H, Stubbs S. Characterization and gene expression profiling of a stable cell line expressing a cell cycle GFP sensor. *Cell Cycle*, **4**(1), (2005), 191-5.

[5] Thomas N. Lighting the circle of life: fluorescent sensors for covert surveillance of the cell cycle. *Cell Cycle*, **2**(6), (2003), 545-9.

[6] Bailly, C. Topoisomerase-I poisons and suppressors as anti-cancer drugs. *Curr. Med. Chem.*, **7**, (2000), 39–58.

[7] Wang, J. C.. DNA topoisomerases. *Annu.Rev. Biochem.*, **65**, (1996), 635–692.

[8] Thomas, N. and I. D. Goodyear. Stealth sensors: real-time monitoring of the cell cycle. *Targets*, **2**, (2003), 26–33.

[9] Feeney, G. P., R. J. Errington, M. Wiltshire, N. Marquez, S. C. Chappell and P. J. Smith. Tracking the cell cycle origins for escape from topotecan action by breast cancer cells. *Br. J. Cancer*, **88**, (2003), 1310–1317.

[10] Lakowicz, J. R., I. D. Fang, Z. Gryczynski, I. Gryczynski and T. G. Burke. Fluorescence spectral properties of the anti- cancer drug topotecan by steady-state and frequency domain fluorometry with one- photon and multi-photon excitation. *Photochemistry & Photobiology*, **69**, (1999), 421–428.

[11] Evans, N. D., R. J. Errington, M. J. Chapman, P. J. Smith, M. J. Chappell and K. R. Godfrey. Compartmental modelling of the uptake kinetics of the anti-cancer agent topotecan in human breast cancer cells. *Int. J. Adapt. Control Signal Process.*, **19**, (2005), 395– 417.

[12] Khan, I. A., J. Fisher, P. J. Smith and R. J. Errington. A Bioinformatics approach for the interrogation of molecular events in single cells: transforming fluorescent timelapse microscopy images into numbers. *BMC Systems Biology* (2007) (*in press*).

[13] AEA Technology, Facsimile (Unix version) User Guide. Harwell Laboratory: Didcot, Oxfordshire, UK, 1994.

Table Legend

Table 1.

Table of parameter values. Where parameters are estimated from the live-cell data SDLN values are provided (in brackets). For the observation parameters α and β different estimates (where appropriate) are obtained before (top) and after (bottom) the second peak.

Table 1

Parameter	**Value**		
k_1	1.5975×10^{-1}		
k_2'	1.5975×10^{-1}		
k_2''	3.9937×10^{0}		
k_3'	3.9937×10^{0}		
k_3''	$3.9937\times10^{+1}$		
k_4	$1.3978\times10^{+2}$		
J_3	0.04		
J_4	0.04		
J_5	0.3		
μ	3.9937×10^{-2}		
m_*	10		
	Control	**1 μM TPT**	**10 μM TPT**
α	68.31 (0.15)	95.88 (0.27) 87.49 (0.38)	110.53 (0.28) 34.17 (1.18)
β	65.79 (0.07) 53.54 (0.07)	40.54 (0.17) 46.06 (0.16)	59.08 (0.12) 36.67 (0.23)
k_2'''	0	0.580 (0.01)	0.414 (0.001)
k_{11}	0	0.666 (0.02)	0.441 (0.02)

Figure Legends

Figure 1:

(a) Human osteosarcoma cells (U-2 OS cells) expressing a cyclin B1-GFP stealth reporter (left panel) and a corresponding transmission image (right panel) to identify all the cells in the field of view. The cells are expressing different levels of cyclin B1-GFP and are hence at all different stages of the cell cycle. (b) Capturing an image every 20 minutes enables single cell tracking, providing a means of continuous cell cycle monitoring for every cell. This provides the experimental data for building and validating the cell cycle model.

Figure 2:

Diagram of the action of topoisomerase I during the cell cycle in (a) the absence and (b) the presence of TPT (after Bailly [2]).

Figure 3:

Schematic of the cell cycle showing the main phases and the *Start* and *Finish* transitions.

Figure 4:

Schematic of the cell cycle showing the *Start* and *Finish* transitions. In addition, the key components of the basic cell cycle model are indicated: cell cycle regulation is controlled by the interaction of cyclin dependent kinases (Cdks) and cyclin B1 with the Anaphase Promoting Complex (APC) group of proteins. APC negates Cdk activity by degrading the cyclin B1 while Cdk/Cyclin B1 inhibits APC activity.

Figure 5:

Schematic of the drug kinetics-cell cycle model. The circular compartments represent variables within the drug kinetics model, which affects the cell cycle model via an indirect inhibition of cyclin B. The coupling involves a signal transduction cascade by which phosphorylation changes in the chromatin environment indicate the magnitude and persistence of lesions.

Figure 6:

The relationship between Cdk-Cyclin B and APC during the cell cycle. At G1, Cdk activity is low and cyclin B1 is rapidly degraded and then at *Start*, cyclin B1 levels are promoted. Cdk levels rapidly rise and are maintained through S, G2 and M while at *Finish*, APC proteins are activated and specific proteins degraded.

Figure7:

Encoded cell lineage with corresponding molecular readout. (a) An exemplar lineage encoded from a real cell using FluroTRAK. Progenitor cell (B) divides into two daughter cells 5 hours after the start of the experiment. The north daughter (BN) again divides at 27.66 hours into two daughter cells BNN and BNS while the south daughter BS failed to divide within the duration of the experiment. Three living cells (BNN, BNS and BS) at the end of the experiment yielded three tracks labelled as track 1 2 and 3 respectively. Continuous cyclin B1-GFP intensity from cytoplasm of track 1 is plotted from the encoded data as an example. (b) Similarly extracted continuous cyclin B1-GFP intensity tracks extracted from typical G2 cells responding to a dose range of topotecan (TPT).

Figure 8:

Model fits showing model predictions (solid lines) and Cyclin B data (dashed lines) against time (*t*), (a) in the absence of TPT, and presence of (b) 1μM and (c) 10μM TPT. An artefact of morphological changes during the final stages of mitosis is the over expression of cyclin B fluorescence giving to false peaks in the experimental data. In an attempt to minimise the impact of this effect the data were capped.

Figure 1a

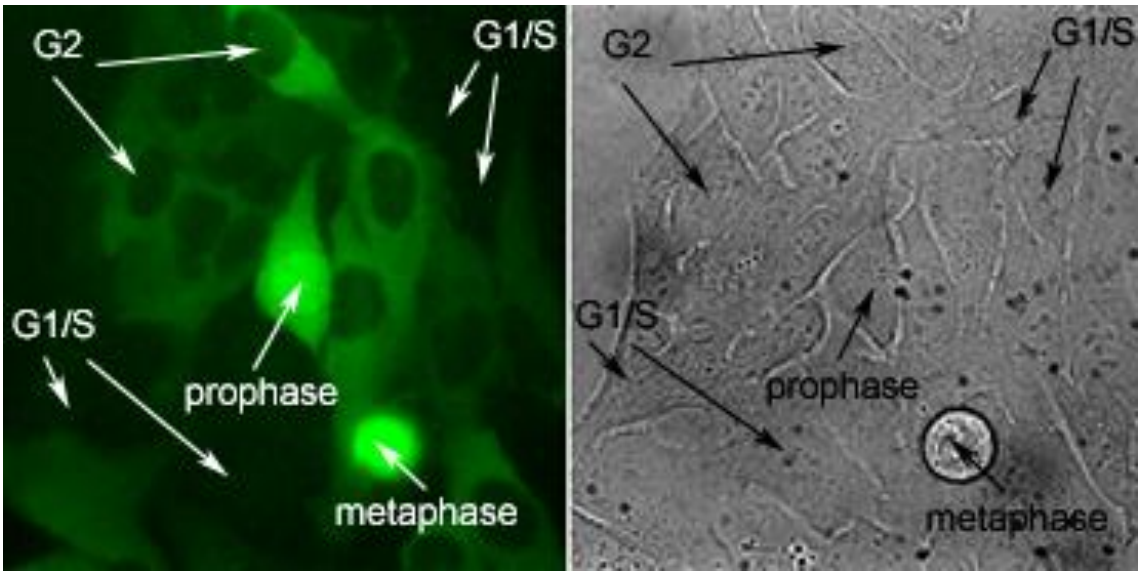

Figure 1b

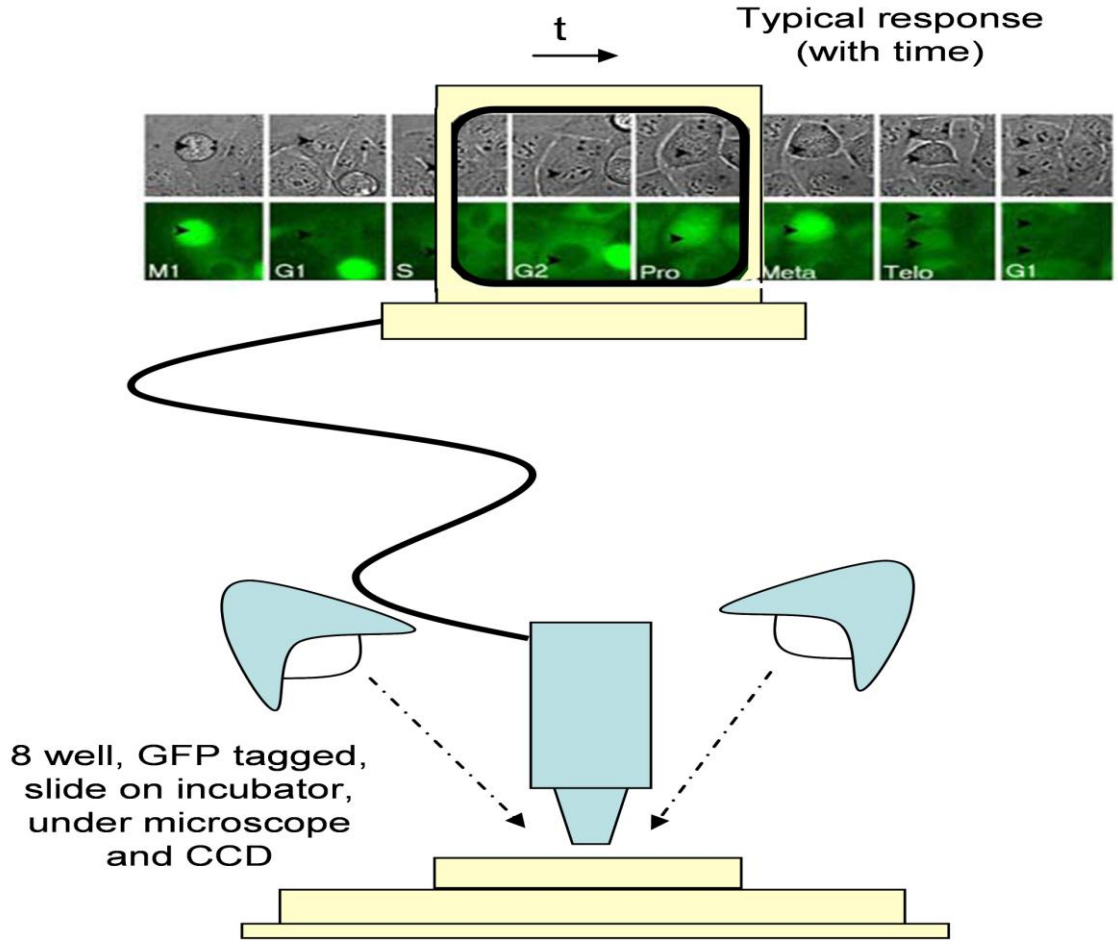

Figure 2

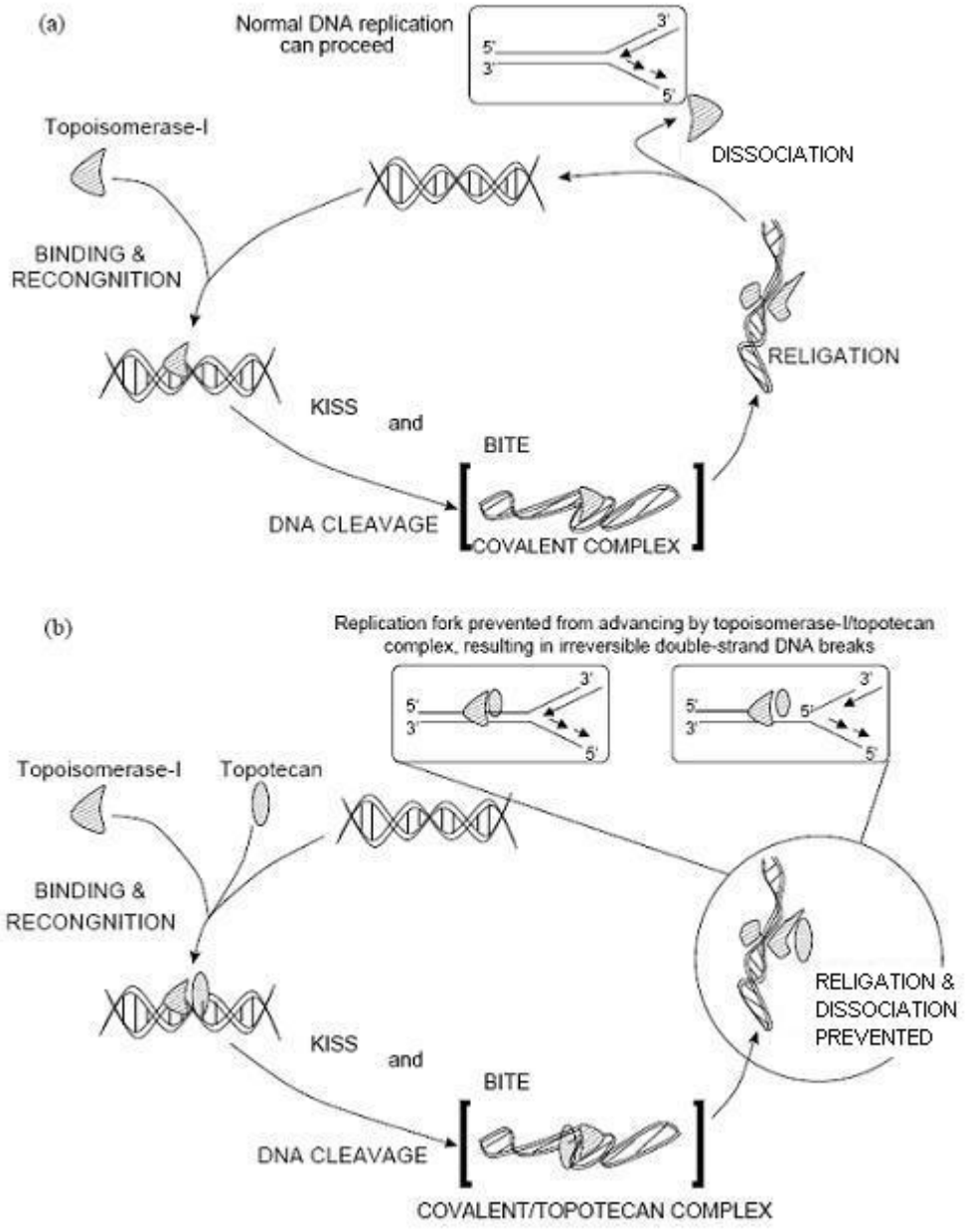
(a)
Normal DNA replication can proceed
3'
5'
3'
5'
Topoisomerase-I
DISSOCIATION
BINDING & RECONGNITION
RELIGATION
KISS
and
BITE
DNA CLEAVAGE
COVALENT COMPLEX
(b)
Replication fork prevented from advancing by topoisomerase-I/topotecan complex, resulting in irreversible double-strand DNA breaks
Topoisomerase-I
Topotecan
BINDING & RECONGNITION
RELIGATION & DISSOCIATION PREVENTED
KISS
and
BITE
DNA CLEAVAGE
COVALENT/TOPOTECAN COMPLEX

Figure 3

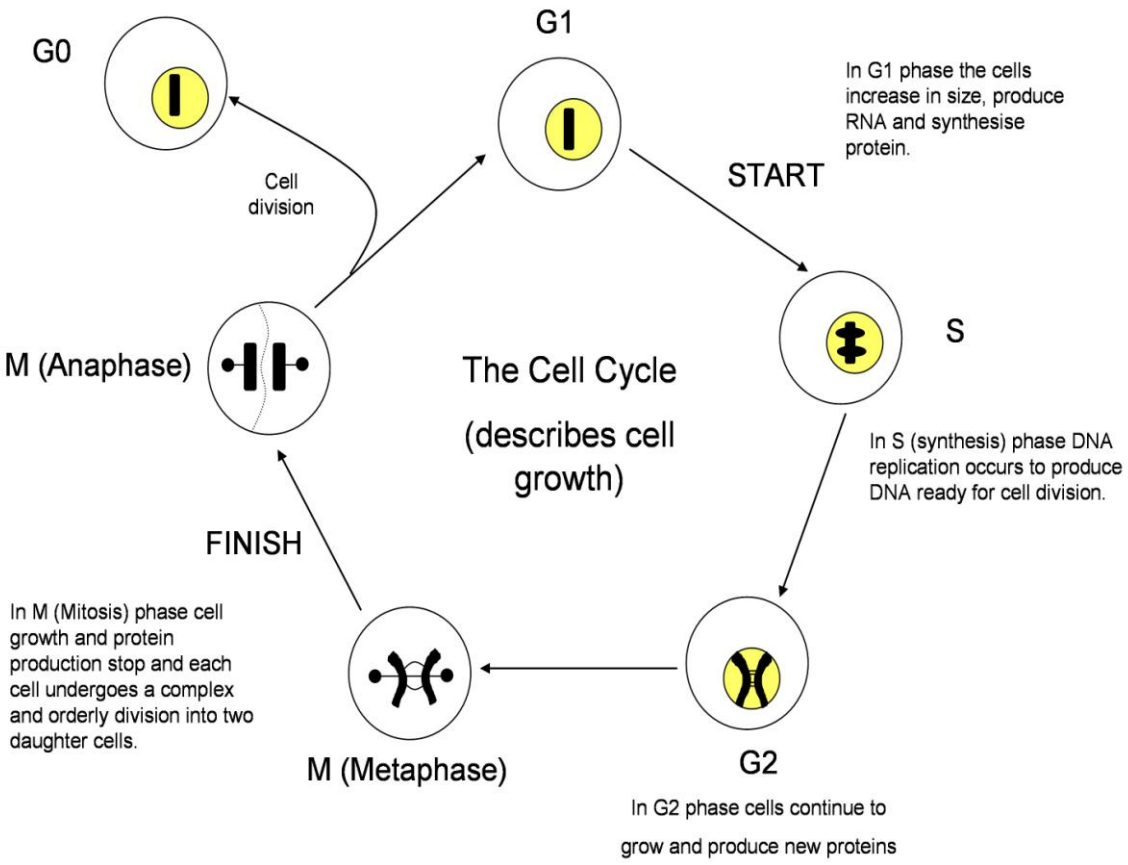
G0
G1
In G1 phase the cells increase in size, produce RNA and synthesise protein.
Cell division
START
S
M (Anaphase)
The Cell Cycle
(describes cell growth)
In S (synthesis) phase DNA replication occurs to produce DNA ready for cell division.
FINISH
In M (Mitosis) phase cell growth and protein production stop and each cell undergoes a complex and orderly division into two daughter cells.
M (Metaphase)
G2
In G2 phase cells continue to grow and produce new proteins

Figure 4

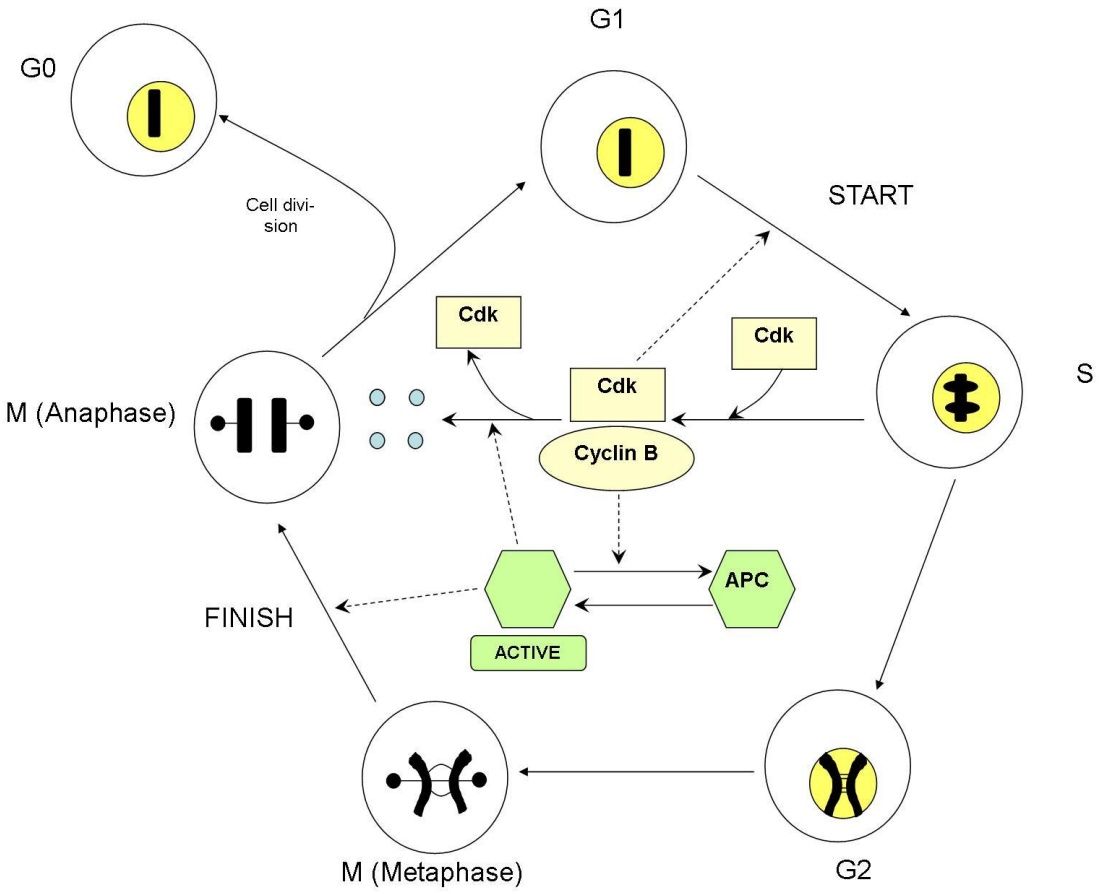
G1
G0
START
Cell divi-
sion
Cdk
Cdk
Cdk
S
M (Anaphase)
Cyclin B
APC
FINISH
ACTIVE
M (Metaphase)
G2

Figure 5

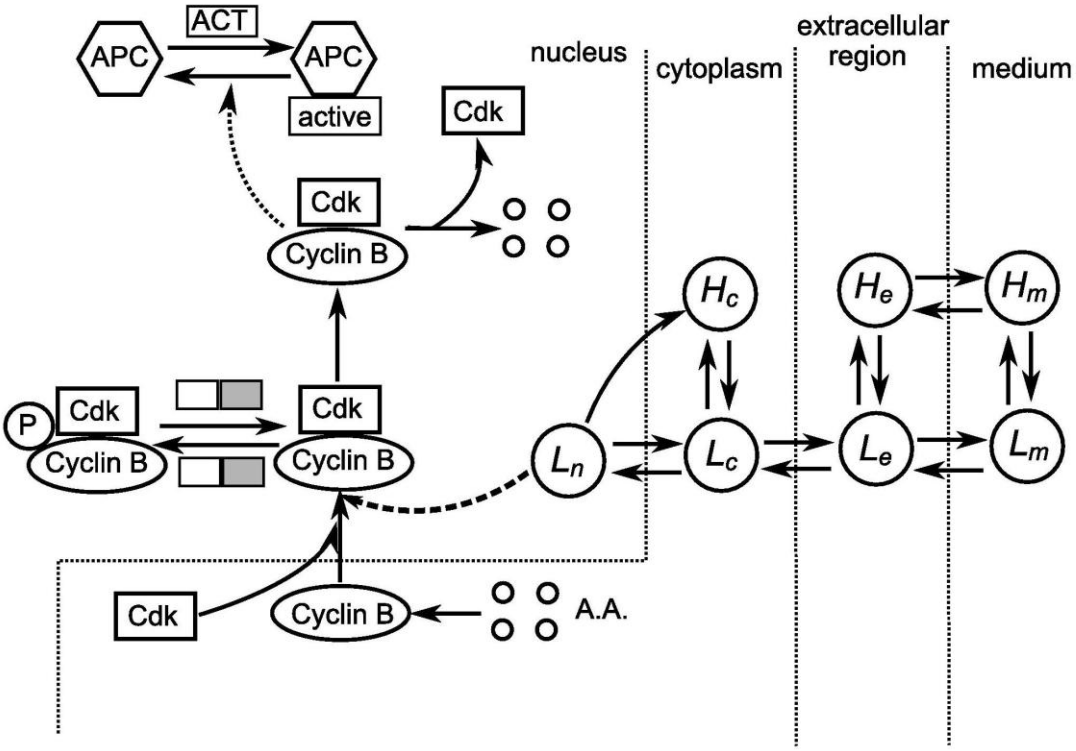
ACT
APC
APC
active
Cdk
Cyclin B
nucleus
cytoplasm
extracellular region
medium
H_c
H_e
H_m
P
Cdk
Cyclin B
L_n
L_c
L_e
L_m
A.A.

Figure 6

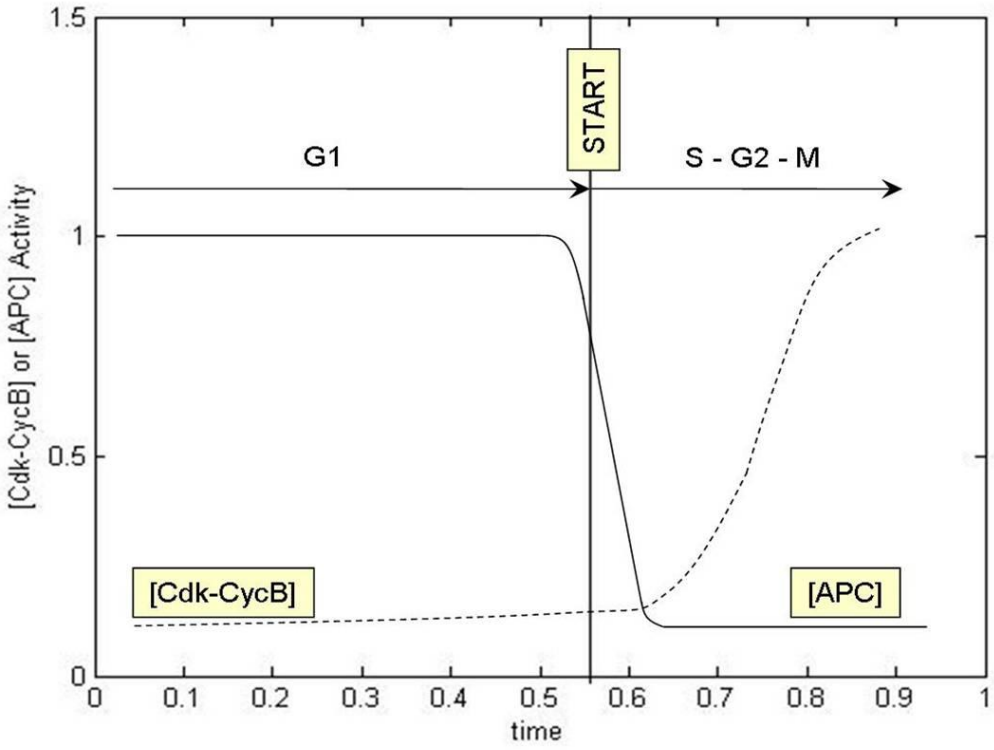
1.5
1
0.5
0
0
0.1
0.2
0.3
0.4
0.5
0.6
0.7
0.8
0.9
1
time
[Cdk-CycB] or [APC] Activity
START
G1
S - G2 - M
[Cdk-CycB]
[APC]

Figure 7a

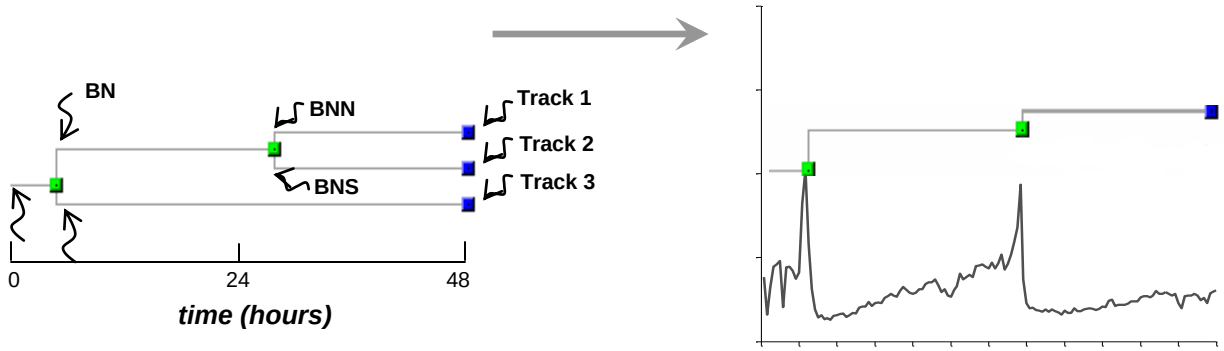

Figure 7b

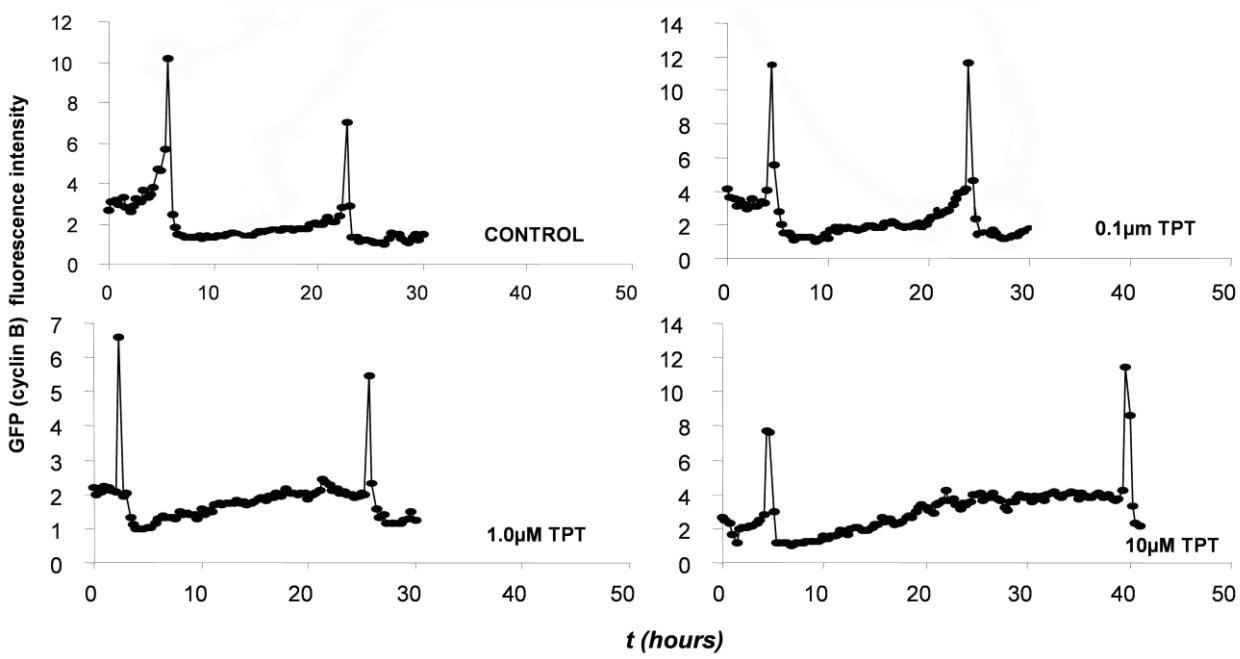

Figure 8(a)

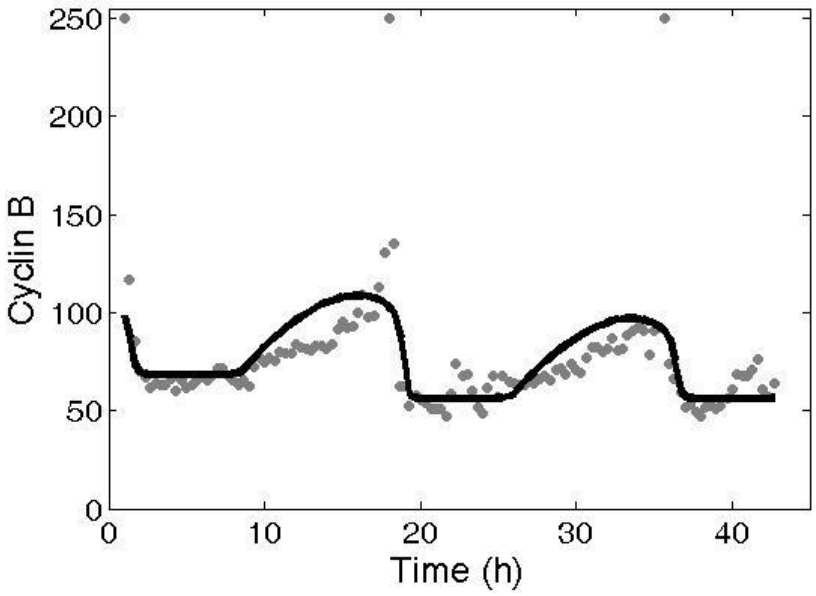

Figure 8(b)

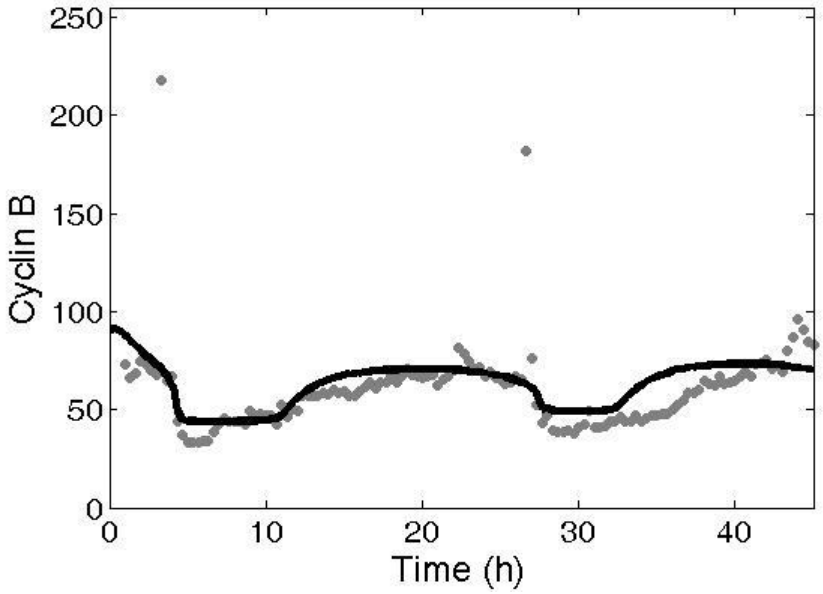

Figure 8(c)